New insights into influencing variables of water atomisation of iron

B. Bergquist

Trace amounts of surfactants have an acute influence on measured surface tension of melts and may influence viscosity. A water atomisation experiment was performed to investigate if variations of these elements could affect quality. Effects of water pressure, melt superheat, and sulphur content, iron scrap oxygen content, and aluminium content were studied. Responses studied were particle size distribution, apparent density, flow, powder chemistry, morphology, green density, and dimensional change. A large sulphur addition reduced the particle size, as a result of a reduction of surface tension, but the largest effect came from changing water pressure. Higher water pressures also resulted in powders with lower apparent density, lower flowrate, and reduced swelling during sintering. An empirical water atomisation model is proposed. Aluminium additions reduced the powder size standard deviation and increased the carbon content of the powder. A reduced powder size standard deviation was seen also for melts with raised superheating. PM/0846

At the time the work was carried out, the author was in the Division of Engineering Materials, Department of Mechanical Engineering, Linköpings universitet, SE–581 83 Linköping, Sweden. He is now with the Division of Quality Technology and Statistics, Department of Business Administration and Social Sciences, Luleå tekniska universitet, SE–971 87 Luleå, Sweden.

© 1999 IoM Communications Ltd.

Published by Maney Publishing (c) IOM Communications Ltd

INTRODUCTION

Producers of iron powder for PM applications strive for a reduction of the impurity content of the powder because of the harmful effects impurities might have on properties such as compressibility, toughness, transverse rupture strength, and hot workability of sintered parts.[1,2] Apprehensions are that reductions to a very low level of surface active contaminants (or surfactants), such as sulphur or oxygen of the melt feedstock for water atomisation, could prove counteractive. The surface tension of iron is increasingly more sensitive to variations of the group VI elements as the content of these approaches zero (Fig. 1).[3–5] Since surface tension is considered a predominant variable in the comminution of a melt, atomisation of occasionally polluted scrap would then result in process disturbances with large batch to batch particle size variations, given that the suspicions regarding surfactants are proved correct.

However, the time taken to form a particle during atomisation is about four or five orders of magnitude smaller than times used to investigate surface tension. The surface/volume ratios seen in melt atomisation and press and sinter size ranges, are typically two orders of magnitude larger than those seen during normal surface tension measuring techniques, such as the sessile drop technique.[6] The surrounding atmosphere of a droplet during sessile drop measurements is dramatically different from the one experienced during atomisation. Thus, it is not self-evident that the same bulk concentration will yield a similar reduction in surface tension.

Nevertheless, a gas atomisation experiment performed by Strauss[7] on copper showed a reduction of particle size by 15% when an otherwise pure melt was doped with 100 ppm sulphur. The reduction was almost 30% when 1000 ppm sulphur was added.[7] Klar and Shafer conducted a water atomisation experiment with copper doped with oxygen, and found a 20% decrease in the particle size for melts saturated with oxygen compared with melts prepared under hydrogen protection.[8] Klar and Fesko also investigated surface tension effects in a water atomisation experiment on copper.[9] In this experiment, the effects of oxygen, silicon, phosphorus, lithium, and magnesium contents on particle formation were investigated. Their results were the opposite of those of Strauss[1] and those of Klar and Shafer.[8] Melts deoxidised with silicon had smaller particle size (oxygen is surface active in copper, silicon is not). Phosphorus added to the copper melt decreased surface tension and increased the resulting particle size. Their conclusion was that a major size effect was an agglomeration of smaller particles.[9] Formed surface compounds would then hinder small particles from joining and agglomerating. Powders atomised from melts with elements prone to oxidation, such as silicon, often have a narrow size distribution. The theory, consistent with agglomeration, was that prevention of agglomeration avoided different parts of the atomisation zone from developing different particle sizes owing to different probabilities of collision.

Surface tension effects

The surface tension of liquid metals under the influence of surfactants and deoxidisers is complex; even correctly measuring the surface tension of mercury at room temperature is difficult, and so measuring at and above the liquidus temperature of iron has no doubt added to the difficulty, as reflected by the large scatter of the published data. Oxygen and sulphur are more active in iron melts than in copper, as stated in previous work.[5] Oxygen is present in the surrounding air, naturally dissolved in water, and may also be catalysed from water molecules decomposed by the liquid melt. The surface tension of iron as a function of oxygen at 1550°C is shown in Fig. 1. The oxygen affinity of alloying elements and the permeability and stability of the formed oxides are also important for the effect of reducing surface tension. If the atomisation chamber is filled with air, the dominant part of the oxygen pickup is seen to evolve from the air contact of the droplets/particles.[10,11]

Sulphur is a strong surfactant in iron, but whether it is more or less active than oxygen is a matter of debate.[4,5] Moderate sulphur additions to an oxygen rich melt might not reduce the surface tension. Melts without oxygen, however, would be greatly influenced by trace amounts of sulphur (Fig. 1). The minimum surface tension measured with sulphur additions is around 0·7 Pa. The minimum surface tension as a result of oxygen in the bulk is above

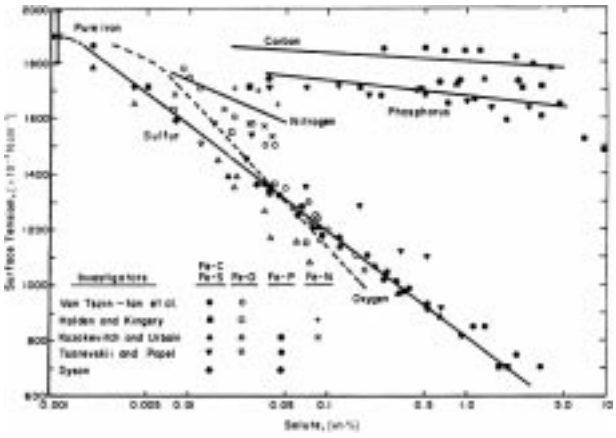

1 Surface tension of iron versus impurity elements (after Ref. 5)

1 Pa.[5,12] Aluminium and silicon, by themselves, should not affect the surface tension of the melt. However, both are strong deoxidisers, and by reducing oxygen they restore the surface tension of oxygen containing melts.[13]

Raised temperatures normally reduce surface tension as the vapour pressure increases (surface tension must equal zero at the critical temperature). However, the temperature coefficient of the surface tension of melt containing oxygen or sulphur is often positive; increases in temperature are followed by increased surface tensions. Binary Fe–O melts change the sign of the temperature coefficient at about 0·002 wt-%O, and Fe–S melts at 0·004 wt-%S.[4] This may be a result of increased evaporation of the surface oxygen or sulphur.

Viscosity effects

Iida and Guthrie[6] proposed that viscosity of a dilute alloy should not be particularly sensitive to small chemical changes, as it is a property of the bulk. Similar observations were made by Bazin *et al.*[14] for an iron melt containing oxygen. There are, however, investigations where viscosity was supposedly greatly affected by the oxygen content.[15] Tsepelev *et al.*[16] also found a large influence of oxygen on the liquid viscosity, which was greatly suppressed in iron melts containing carbon. Similar observations were made by Bodakin *et al.*[17] who found that at about 0·3 wt-%C, oxygen content had no influence on viscosity.

There are investigations where trace amounts of sulphur would considerably lower viscosity. An iron melt, with a sulphur content of 100 ppm would, according to Frohberg and Cakici,[18] have 6% lower viscosity at 1550°C than a melt with only 10 ppm sulphur. The minimum viscosity obtained for melts containing 0·1 wt-%S is 18% lower than for pure iron melts. Addition of aluminium to deoxidise the melt may slightly increase the viscosity, as alumina particles form.

Prior conclusions regarding physical properties

Small variations of scrap metal impurities are inevitable as deoxidising is common practice and temperature may vary. It is therefore of interest to verify the effects of such actions for water atomisation of iron. The discrepancies seen when investigating the physical properties of the iron melt are most likely a result of the difficulty of measuring correctly at the high temperatures involved, together with the problem of keeping the melts pure. Understandably, if it is difficult to even measure properties during experimental conditions, it would be almost impossible to keep them stable in a nearly pure melt in an industrial environment. A validation experiment was therefore performed in order to increase the experimental data regarding the importance of impurities and deoxidising practice on the powder properties of water atomised iron powder.

EXPERIMENTAL

Experimental facility and general procedure

A modified Davy McKee D5 15 kg atomiser, located at the Höganäs laboratory, was used to perform the validation experiment. The atomiser has an induction heated alumina ladle that contains a stopper rod to allow for bottom tapping through an 8 mm diameter nozzle. The ladle is emptied into a graphite tundish which has a nozzle with a diameter of 6 mm. Propane torches heat the tundish red hot. The atomisation zone consists of two primary and two secondary water jets in a closed V jet configuration, with angles of 25 and 15° between jets and melt stream respectively (Fig. 2).

The charge weight was 7 kg and the charges contained 0·4 wt-% graphite, added as 10 g graphite and 40 g ASC 100.29 iron powder compacts. During the investigation, distilled water was used as the atomisation medium, and the water pressure was set by water jet changes. Total water flow was constant at 0·92 L s^{-1} during the experiment as a displacement pump was used. The main/secondary water jet configuration was selected so that main/secondary water flow proportions remained constant. The atomising chamber was purged with nitrogen and the powder collected after settling for 60 min. A vacuum oven, heated to 110°C, was used to dry the powder. The coarsest fraction of the dry powder (presumably a result of splashing of melt out of the atomising zone) was sieved off with a US standard sieve no. 35, with a sieve opening of 500 μm. The equipment and measurements used are given in Table 1. Subsequently powders from atomisations F74–F92 (Table 2) were reduced, admixed with copper and graphite (*see* Table 3), and then sintered to investigate dimensional change.

Variables and ranges

It is well known that high water velocities reduce the particle size of the atomised powder, and this was selected to compare water velocity to other less investigated variables. The water velocity is proportional to the square root of the water pressure, and as pressure was measured already, this variable was chosen as a measure of water velocity. The selected levels of water pressure p are seen in Table 2. Crucible melt temperature T is a variable that will affect the physical properties of the powder and it was also investigated (Table 2).

Surfactant behaviour was investigated partly through sulphur additions to the melt and partly using a melt

Table 1 Analysis equipment and procedures

Iron powder particle size	ISO 4497, dry sieving; ISO 565 T.2
Flow	ISO 4490:1978
Apparent density	ISO 3923–1:1979
Dimensional change	ISO 4492:1993; testpiece ISO 2720:1973
SEM analysis	JEOL 6400 SEM; acceleration voltage: 25 keV
XPS and ESCA analysis	VG SCIENTIFIC Microlab 310–F; acceleration voltage: 25 keV
C and S content analysis	LECO CS 345 IR CO_2
O and N content	LECO TC 136

Published by Maney Publishing (c) IOM Communications Ltd

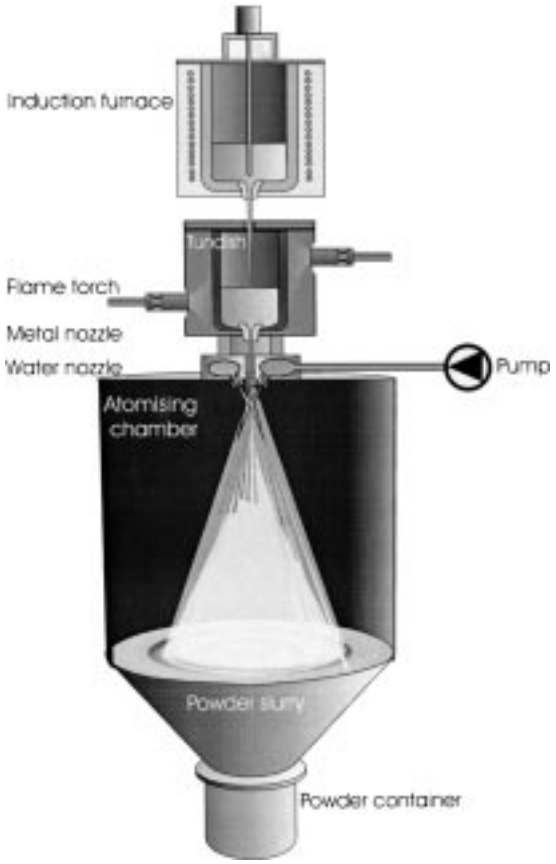

2 Outline of atomisation facility: metal is melted in bottom emptied induction furnace, poured via tundish into atomisation zone where water jets disintegrates melt stream

practice thought to induce or avoid oxygen in the melt. The sulphur content was varied in four levels, no addition, or additions of 0·1, 0·2, or 1·5 wt-% respectively. The large surface/volume ratios of the experimental melts were expected to enhance sulphur evaporation and large additions assured that some sulphur would be present even if some evaporated. Therefore, the added sulphur levels of 0·1 and 0·2 wt-% are larger than levels that are ever expected in production. The 1·5 wt-% level was chosen to see how the atomisation reacted to extreme contents. The sulphur was added as FeS, approximately 30 s before melt release.

Table 2 Experimental design*

Run label	*S*, wt-%	*T*, °C	*p*, MPa	Pure iron fraction	*A*, wt-%
F074	0·2	1602	15·5	0·91	0·02
F081	0·2	1616	15·5	0·52	0
F082	0·002	1576	15·5	0·51	0
F083	0·001	1650	15·5	0·98	0·02
F084	0·001	1570	10·5	0·98	0·02
F085	0·2	1570	10·5	0·52	0
F087	0·2	1656	10·5	0·97	0·02
F091	0·002	1643	10·5	0·48	0
F092	0·1	1610	12·5	0·77	0·01
F100	0·002	1640	12·5	0·49	0
F101	0·001	1644	12·5	0·98	0·02
F102	1·5	1646	12·5	0·95	0·02
F103	0·003	1648	12·5	0·39	0·02

* *S* is predicated S value, *T* is crucible melt temperature, *P* is water pressure, and *A* is predicted Al value.

The effects of oxygen and deoxidising practice were investigated with two variables: aluminium content and pure iron fraction. Melts with supposedly high oxygen level were produced by melting approximately 3·5 kg pure iron blocks along with the graphite containing compacts under argon atmosphere, and then adding close to 3·5 kg of unreduced Höganäs ASC type powder without argon protection. These melts were not aluminium deoxidised. Low oxygen levels were produced by melting close to 7 kg of pure iron blocks plus graphite containing compacts under argon atmosphere and then deoxidising the melts with 0·02 wt-%Al for approximately 30 s before melt release, with one exception which is mentioned below. Pure iron fraction is defined as the fraction of iron in the melt originating from pure iron. The oxygen contents of the melts were not measured, but the high oxygen content melts were notably more effervescent, an indication of a higher oxygen content. In order to separate a potential effect of impurities in the unreduced ASC powder compared with the pure iron melts, one melt (F103) was molten with switched charge order. That is, initial melting was performed with ASC powder under a protective atmosphere, followed by final scrap addition of pure iron blocks still protected by argon, and then deoxidised with aluminium. It was thought that this procedure would ensure that oxygen content of this melt was low, but still contained impurities from the ASC powder. Subsequent analysis of the resulting powder was performed with equipment according to Table 1.

Experimental design and evaluation

The experimental design chosen is given in Table 2. Originating as a 2^{4-1}_{IV} factorial designed experiment with one centre point experiment (runs F74–F92), four extra runs (F100–F103) were added to increase the experimental space spanned and to separate the possible predictor variable confounding (Table 2). The run order is indicated by the run name. The correlation between predictor variables are given in Table 4. The correlation between pure iron fraction and aluminium content is large (0·77), and this is because they were varied in the same pattern, with the exception of run F103.

Before analysis, the independent variables were centred and scaled to unit variance. In classical regression, the responses $(y_1, y_2, ..., y_n)$ are assumed to be a function of a mean and a continuous function of the predictor variables x_i and a random error ε owing to measurement errors and unconsidered effects, that is, the observations can be fractionated into

$$y_1 = \beta_0 + \beta_1 x_{11} + \cdots + \beta_r i_{1r} + \varepsilon_1$$
$$y_2 = \beta_0 + \beta_1 x_{21} + \cdots + \beta_r x_{2r} + \varepsilon_2$$
$$y_n = \beta_0 + \beta_1 x_{n1} + \cdots + \beta_r x_{nr} + \varepsilon_n$$

or in matrix form $y_{(n\times 1)} = X_{[n\times(s\times 1)]}\beta_{[(s+1)\times 1]} + \varepsilon_{(n\times 1)}$, where y is the response vector, X is the experimental design matrix with the corresponding values of the predictor variables, β is the vector of unknown predictor coefficients, ε is the error vector, n is the number of observations, and s is the number of predictors. The best prediction of the responses would use all of the information of the estimation of the predictor coefficients $\hat{\beta} = (X^T X)^{-1} X^T y$.

Experimental considerations

The original intention was to test a wider range of crucible melt temperatures than seen in Table 2. A higher temperature was however difficult to reach owing to nozzle and stopper rod failures and lower temperatures led to severe freezeups of the tundish. The melts were released when the predetermined temperature was reached, as measured by a thermocouple within the stopper rod. The narrower

Published by Maney Publishing (c) IOM Communications Ltd

Table 3 Resulting physical powder properties*

Run label	μ_P, μm	σ_P	Flow, s	AD, g cm^{-3}	D, %	σ_D, %	Iron flow, kg s^{-1}	Water to iron mass flow	C, wt-%	S, wt-%	O, wt-%	N, wt-%
F074	59·5	2·36	23·9	3·32	0·47	0·009	...	...	0·06	0·187	0·33	0·015
F081	62·2	2·51	23·4	3·46	0·51	0·009	...	...	0·11	0·187	0·34	0·021
F082	74·7	2·64	24·1	3·43	0·45	0·003	...	...	0·15	0·009	0·42	0·029
F083	51·9	2·17	24·8	3·16	0·43	0·005	...	...	0·31	0·006	0·37	0·015
F084	99·2	2·36	18·7	4·01	0·60	0·004	...	...	0·32	0·007	0·23	0·012
F085	111·3	2·44	18·2	4·11	0·62	0·016	...	...	0·14	0·184	0·55	0·069
F087	91·3	2·31	17·5	4·20	0·61	0·012	...	...	0·27	0·176	0·23	0·014
F091	100·2	2·34	19·4	4·03	0·61	0·010	...	...	0·18	0·008	0·44	0·036
F092	74·1	2·37	24·5	3·41	0·58	0·013	...	...	0·24	0·091	0·32	0·023
F100	68·2	2·50	24·26	3·32	...	...	~0·18	~5·1	0·02	0·008	0·57	0·014
F101	82·4	2·32	20·16	3·67	...	...	0·204	4·5	0·31	0·006	0·46	0·013
F102	54·0	2·30	21·55	3·32	...	...	0·200	4·6	0·28	0·988	0·87	0·012
F103	67·7	2·30	22·88	3·43	...	...	0·174	5·3	0·26	0·011	0·41	0·015

* μ_P is mass median particle size, σ_P is size distribution standard deviation, AD is apparent density, D is dimensional change, and σ_D is dimensional change standard deviation.

temperature range led to some difficulties. The temperature was difficult to adjust precisely and the temperature deviation from target was in one instance 24°C. A larger temperature range would, of cause, have reduced the relative error.

The experimental design is not orthogonal, partly because of the practical difficulties of setting correct temperature and partly owing to the fact that the extra experimental runs included to increase information were to few to obtain orthogonality. A confounding, or multicollinearity of the predictor variables is therefore expected. The remedy of situations where multicollinearity is serious is to delete one or several of the predictor variables, or to use regression methods such as ridge regression.[19–21] Ridge regression is controversial and should be used cautiously. A check of the severity of the multicollinearity can be performed in several fashions. The correlation matrix (X^TX where X is the scaled and centred design matrix) should be checked (Table 4). The correlation matrix of an orthogonal experimental design is the identity matrix, with all eigenvalues being equal to one. If a variable is confounded on several variables, the correlation matrix might not reveal any large correlations between single variables. A check of the eigenvalues λ corresponding to the correlation matrix is insensitive to such confoundings.

The collinearity is measured by the condition number $\phi = \lambda_{max}/\lambda_{min}$ and as a rule of thumb, if $\phi > 1000$, one should be concerned.[21] For this design matrix (the eigenvalues of the correlation matrix (Table 4) are 0·90, 0·83, 1·01, 0·20, and 2·06) $\phi = 10{\cdot}2$. Other measures of collinearity are the variance inflation factors (VIFs). The VIF measures the collinearity of a variable with respect to the others. A VIF is the diagonal element of the inverse of the correlation matrix, subsequently used for predictor coefficient calculations. As a rule of thumb, a VIF >10 is a reason for some concern.[21] The largest VIF is 2·79 (Table 5) indicating that the collinearity of the experiment is small. Nevertheless, the collinearity might be reduced if one of the predictor variables was excluded, and a sequential procedure of selecting the important variables for the regression was used.

Table 4 Correlation matrix of independent variables

	S, wt-%	T, °C	p, MPa	Pure iron fraction	A, wt-%
S, wt-%	1	0·18	−0·03	0·29	0·24
T, °C	0·18	1	−0·04	0·14	0·34
p, MPa	−0·03	−0·04	1	0·00	−0·03
Pure iron fraction	0·29	0·14	0·00	1	0·77
A, wt-%	0·24	0·34	−0·03	0·77	1

The selection criterion determined if the predictor variable in combination with other selected variables increased or reduced the sum of residual variation for all scaled and centred responses obtained from all experiments (Table 6). The smallest sum of residual variance was obtained when all variables except pure iron fraction were included; without pure iron fraction, the largest VIF decreased to 1·17 and ϕ to 1·82 (the eigenvalues of the correlation matrix without pure iron fraction is 0·99, 0·83, 0·66, and 1·52). Thus, adding the pure iron fraction variable does not reveal much information about the results of the experiment, and with the pure iron variable correlation with aluminium content, it adds collinearity. The pure iron fraction was therefore excluded from further regression.

RESULTS

Each response was measured twice and the arithmetic mean presented in Table 3 was used for the experimental evaluation. The particle size distribution is presented as mass median particle size μ_P and size distribution standard deviation σ_P defined as $\sigma_P \equiv d_{84{\cdot}13}/d_{50}$. Dimensional change was measured on five tensile specimens from run F74 to F92. The tensile specimens were produced from reduced powder, compacted at 600 MPa with 2 wt-%C, 0·5 wt-% graphite, and 0·5 wt-%Zn stearate added, and both the averages and the standard deviations are presented in Table 3.

Calculations for the analysis of variables are based on the scaled and centred predictor variable matrix X. The sum of square for the predictor coefficients is calculated as the sum of squared indices of the vector $\hat{\beta}_i X_i$, where $\hat{\beta}_i$ is the ith predictor coefficient and X_i the ith column of X obtained from $\hat{\beta} = (X^TX)X^Ty$ and y is the response vector. Note that the sum of squares SS_β for the predictor coefficients together with the residual sum of squares SS_R does not equal the total sum of squares, obtained from y. This is a result of the multicollinearity still existing in the design matrix and the difference is found in the row collinearity. The error is made when viewing the predictor coefficients as single coefficients, rather than unanimously.

Table 5 Variance inflation factors

	S, wt-%	T, °C	p, MPa	Pure iron fraction	A, wt-%
VIF*	1·12	1·21	1·00	2·63	2·79
VIF†	1·07	1·14	1·00	...	1·17

* Based on all predictor variables.
† Based an all predictor variables except pure iron fraction.

Published by Maney Publishing (c) IOM Communications Ltd

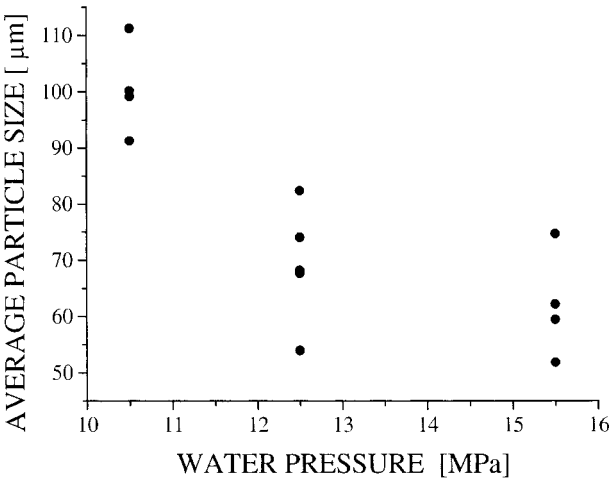

3 Resulting particle size versus water pressure

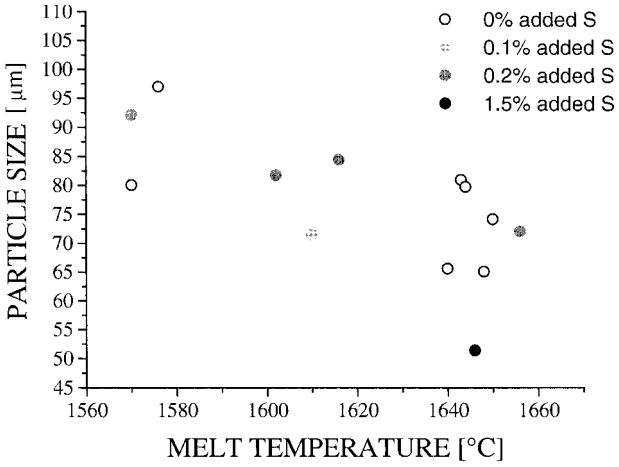

4 Estimated particle size, adjusted for water pressure, versus melt temperature

The residual error is used to test the null hypothesis that the coefficients are equal to zero.

With the remaining predictor variables, the prediction variable matrix X is nearly orthogonal, and thus the error made when predictor coefficients are considered independent of each other is small. For example, the predictor coefficient for the water pressure variable μ_P when estimated separately is equal to $-14{\cdot}84$ and $-15{\cdot}31$ when all predictor variables are evaluated jointly.

The null hypothesis, against which the variables have been tested, is H_0; the predictor variable x_i has no effect, and the corresponding predictor coefficient $\hat{\beta}_i$ is a measure of random error. Confidence intervals of 95% for the prediction estimates are given as $\hat{\beta}_i \pm t_{0{\cdot}025} \times \text{SE}$ (SE is standard error). Here $t_{0{\cdot}025}$ is the tail area probability point 0·025 in a Student's t table with degrees of freedom according to the corresponding error estimate. Predictor coefficients where this interval does not include zero or where zero is just barely included are further examined. The predictor coefficients for predictor variables in Tables (7)–(16) are scaled and centred to unit variance. If their signs seem reasonable, they are considered active.

Particle size results

Water pressure was the most influential variable regarding median particle size (Fig. 3 and Table 7) but the null hypothesis was also rejected for melt temperature and sulphur content. Figure 4 shows the estimated particle size, when the effect of water pressure has been removed, plotted versus atomising temperature. The temperature effect seems reasonable and also follows observations of other researchers.[22] It is therefore considered real. Although being smaller than expected, the sulphur effect also follows presumptions and is considered active. In Fig. 5, the estimated particle size when the effects of temperature and water pressure have been removed, is plotted versus sulphur content.

The residuals $\hat{\varepsilon} = y - \hat{y}$ were estimated according to $y - \hat{y} = y - \beta_1 X_1$. The residuals for μ_P plotted versus run number are shown in Fig. 6. In units for the variables as in Table 2, the equation for μ_P in micrometres is

$$\mu_P = 76{\cdot}67(\pm 4{\cdot}87) - 7{\cdot}43(\pm 2{\cdot}46)(p - 12{\cdot}81) - 0{\cdot}197(\pm 0{\cdot}157)(T - 1621) - 12{\cdot}60(\pm 12{\cdot}51)(S - 0{\cdot}187) \quad . \quad . \quad . \quad . \quad . \quad (1)$$

Table 6 Best predictor choices for given number of predictors

Number of predictor variables	Best predictor variables	Residual sum of squares	Residual degrees of freedom	Sum of residual variance
0	Average	96	12	8
1	Average, p	69·75	11	6·32
2	Average, p, T	58·6	10	5·86
3	Average, p, T, S content	39·70	9	4·41
4	Average, p, T, S content, Al content	26·19	8	3·27
5	Average, p, T, S content, Al content, pure iron fraction	25·16	7	3·59

Table 7 Analysis of water pressure (MPa) variance

μ_P	Degrees of freedom	Predictor coefficient	Sum of squares	Mean squares	F ratio	Probability level	$t_{0{\cdot}0258} \times \text{SE}$
Mean	1	76·67	76 416	76 416	1318·9	0·000	4·868
Sulphur	1	−5·10	312	312	5·4	0·049	5·067
T	1	−6·35	484	484	8·4	0·020	5·067
p	1	−15·29	2805	2805	48·4	0·000	5·067
Aluminium	1	−2·44	71	71	1·2	0·300	5·067
Residual	8		464	57·94			
Collinearity			167				
Total			80 718				

Published by Maney Publishing (c) IOM Communications Ltd

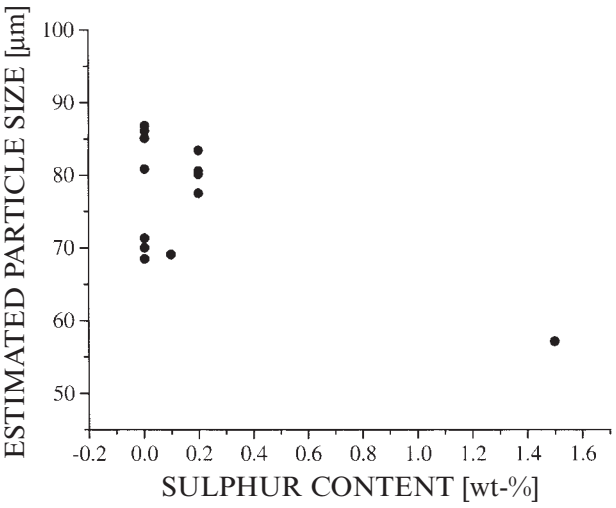

5 Estimated particle size, adjusted for water pressure and melt temperature, versus sulphur content

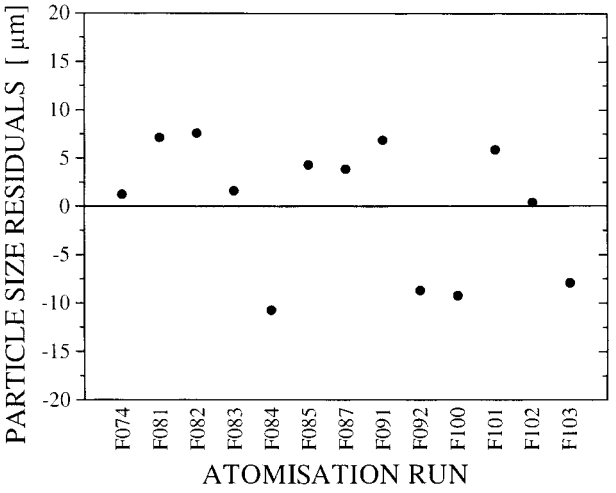

6 Particle size residuals

The average difference between two replicate measures of mass median particle size was 4·37 μm, so the average measurement error for one measurement would be approximately $(4{\cdot}37^2/2)^{1/2} = 3{\cdot}1$ μm. The error of the mean value of two measurements would be $(3{\cdot}1^2/2)^{1/2} = 2{\cdot}19$ μm. The deviation of the residuals from zero, is on average, 6·0 μm; there are therefore other errors or effects with a total size of $(6{\cdot}0^2 - 2{\cdot}19^2)^{1/2} = 5{\cdot}6$ μm unaccounted for by the predictor coefficients.

Particle size distribution standard deviation results

One predictor coefficient, aluminium content, is large enough to be considered active regarding particle size

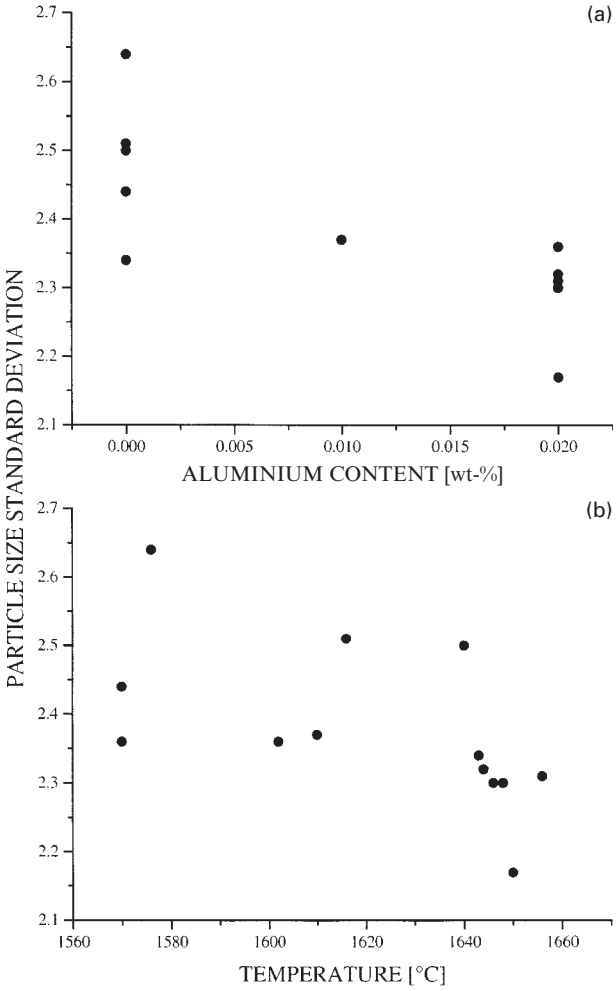

7 Particle size standard deviation versus *a* aluminium content and *b* temperature

standard deviation (Table 8). Nevertheless, the two largest predictor coefficients, the second being melt temperature, deserve a closer inspection (Fig. 7) where both seem active. The conclusion is that aluminium additions and increased melt temperatures reduce particle size standard deviation.

Apparent density, flowrate, and morphology results

The flowrate and apparent density (Tables 9 and 10) are measures largely influenced by powder morphology, as well as by powder size. Powders from runs F74–F92 and F102 were examined by SEM and (Fig. 8) images of powders from two of the melts using high and low water pressure are shown. Powders manufactured at low water pressure had larger, but also more spherical particles.[23] The other variable settings did not noticeably change the morphology. Agglomerates of smaller particles seem to build up large

Table 8 Analysis of particle size distribution standard deviation (μm) variance

σ_P	Degrees of freedom	Predictor coefficient	Sum of squares	Mean squares	F ratio	Probability level	$t_{0{\cdot}0258} \times$ SE
Mean	1	2·38	73·542	73·542	12464·7	0·000	0·049
Sulphur	1	0·01	0·001	0·001	0·2	0·691	0·051
T	1	−0·04	0·022	0·022	3·7	0·090	0·051
p	1	0·02	0·006	0·006	1·0	0·343	0·051
Aluminium	1	−0·08	0·070	0·070	11·9	0·009	0·051
Residual	8		0·047	0·0059			
Collinearity			0·024				
Total			73·712				

Published by Maney Publishing (c) IOM Communications Ltd

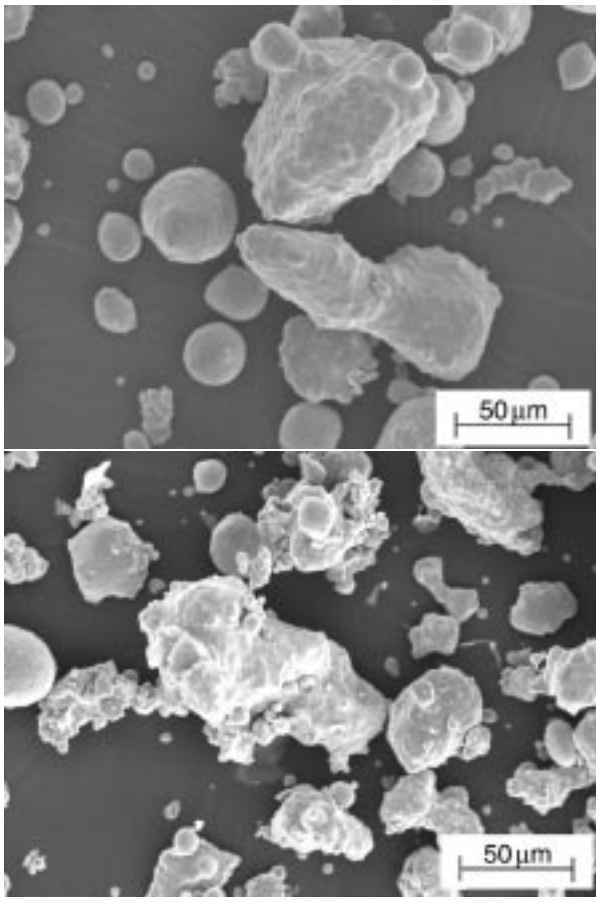

a F84, low water pressure; *b* F74, high water pressure

8 Micrographs of powders from two melts

particles, and this was especially true for high water pressure runs.

Apparent density and powder flowrate were influenced only by water pressure; high pressures decreased both. Note that the apparent density in Table 10 was neither influenced by composition nor temperature, a further

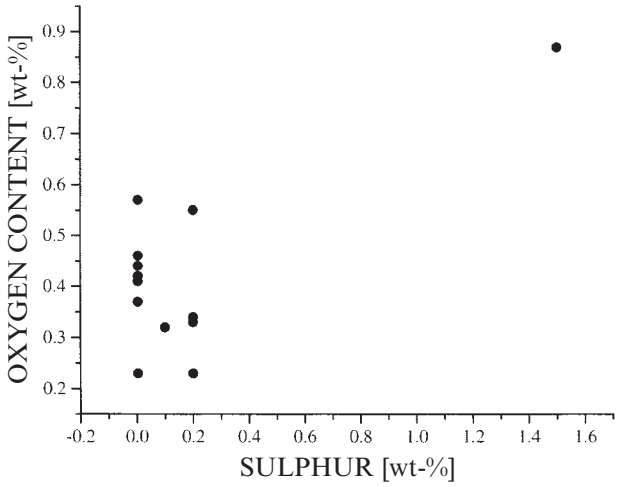

9 Powder oxygen content versus sulphur additions

support for the visual observation that the morphology was unaffected by these variables. The shape of powders manufactured during run F102 (1·5 wt-%S) was comparable to the shapes of powders from other runs. However, the oxygen scale on the powders was notably thicker.

Powder chemistry results

The sulphur content of the powders followed the pattern of the sulphur additions, and showed that only a small fraction (23%) had evaporated, been removed by the atomisation water, or remained as slag on crucible walls. The only predictor variable influencing sulphur content of the powder was the sulphur content variable (Table 11). High oxygen contents of the powder correlated with high sulphur additions (Fig. 9 and Table 12).

Regarding the carbon and nitrogen content of the powder (Tables 13 and 14), the null hypothesis failed for the aluminium addition predictor coefficient. Aluminium additions correlated with lower content of nitrogen and increased content of carbon (Fig. 10). The carbon value observed for F74 deviates with 0·02 wt-%Al from the contents of the other runs. Sieved size fractions analysed

Table 9 Analysis of flow (s) variance

Flow	Degrees of freedom	Predictor coefficient	Sum of squares	Mean squares	*F* ratio	Probability level	$t_{0·0258} \times$ SE
Mean	1	21·79	6174·6	6174·6	1937·3	0·000	1·142
Sulphur	1	−0·11	0·1	0·1	0·0	0·864	1·188
T	1	0·42	2·2	2·2	0·7	0·430	1·188
p	1	2·20	58·3	58·3	18·3	0·003	1·188
Aluminium	1	−0·35	1·5	1·5	0·5	0·512	1·188
Residual	8		25·5	3·1872			
Collinearity			−1·4				
Total			6260·8				

Table 10 Analysis of apparent density (μm) variance

Apparent density	Degrees of freedom	Predictor coefficient	Sum of squares	Mean squares	*F* ratio	Probability level	$t_{0·0258} \times$ SE
Mean	1	3·61	168·98	168·98	3206·5	0·000	0·147
Sulphur	1	−0·06	0·04	0·04	0·8	0·409	0·153
T	1	−0·07	0·06	0·06	1·1	0·317	0·153
p	1	−0·29	1·00	1·00	19·0	0·002	0·153
Aluminium	1	−0·01	0·00	0·00	0·0	1·000	0·153
Residual	8		0·42	0·0527			
Collinearity			−0·01				
Total			170·50				

Published by Maney Publishing (c) IOM Communications Ltd

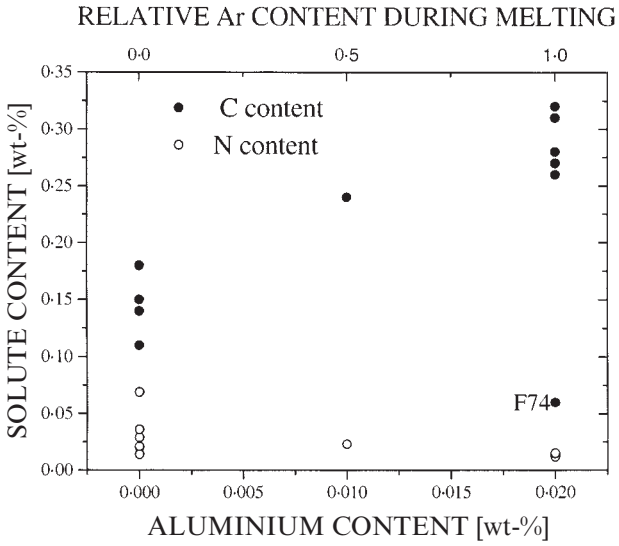

10 Carbon and nitrogen content versus aluminium content

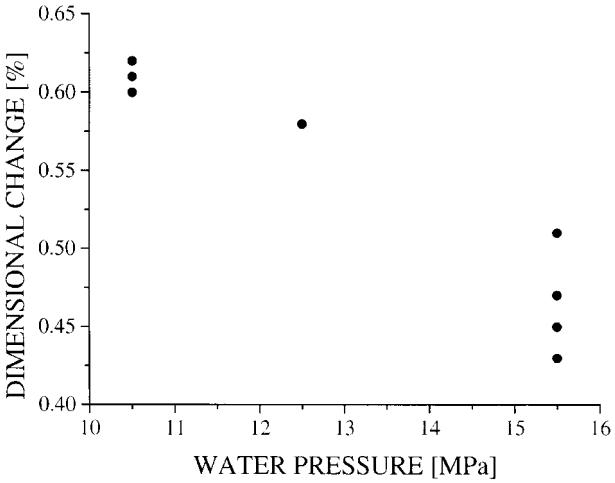

11 Dimensional change versus water pressure

for aluminium, carbon, sulphur, oxygen, or nitrogen only showed an increase in oxide content for small particle sizes, indicating that only oxygen was accumulated on the surface. This was later verified by AES and XPS measurements.

Dimensional change results

The predictor coefficients for dimensional change are found in Table 15; dimensional change was only measured for reduced powders F74–F92. High pressure atomisations decreased dimensional swelling during sintering (Fig. 11). Sulphur additions correlated with an increased dimensional change standard deviation (Fig. 12 and Table 16).

DISCUSSION

Particle size results

Water pressure

The present results may be used to compare presented formulae found in the literature. An often stated formula is

$$\mu_p = k p_w^{-m} \quad . \quad . \quad . \quad . \quad . \quad . \quad . \quad . \quad . \quad . \quad . \quad (2)$$

where p_W is water pressure, and k and m are constants specific for material and plant; m is normally 0·6–0·8.[22]

Ternovoy has presented a mathematical model relating surface tension and viscosity to particle size.[24]

$$\mu_p = k \frac{v_M^{0.35} G_M^{1.24}}{\gamma_M^{0.15} D_M^{1.03} \rho_M^{0.56} \rho_W^{0.25} v_W^{0.07} u_W^{0.96} \sin(\alpha)^{0.96} G_W} \quad . \quad . \quad (3)$$

where indices M and W indicate metal and water respectively, D is melt stream diameter (m), v is viscosity ($m^2\ s^{-1}$), ρ is density ($kg\ m^{-3}$), γ is surface tension ($N\ m^{-1}$), G and u are mass flowrate ($kg\ s^{-1}$) and velocity ($m\ s^{-1}$) respectively, and α is the apex angle.

An empirical model was presented by Kishidaka[25]

$$\mu_P = k \left[\frac{D_M \rho_M (u_W - u_M)}{v_M}\right]^{-0.57} \left[\frac{D_M \rho_M (u_W - u_M)^2}{\gamma_M - \gamma_W}\right]^{-0.22} \times \left(\frac{G_W}{G_M}\right)^{-0.043} \quad . \quad . \quad . \quad . \quad . \quad . \quad . \quad . \quad . \quad (4)$$

The models by Grandzol and co-workers have often been quoted, first presented as particle size being merely a function of a constant, divided by water jet velocity.[26–28] The model was later modified to acknowledge the impact

Table 11 Analysis of sulphur (wt-%) variance

S	Degrees of freedom	Predictor coefficient	Sum of squares	Mean squares	F ratio	Probability level	$t_{0.0258} \times$ SE
Mean	1	0·144	0·2684	0·268	393·5	0·000	0·017
Sulphur	1	0·267	0·8556	0·856	1256·8	0·000	0·017
T	1	−0·006	0·0004	0·000	0·0	1·000	0·017
p	1	0·002	0·0001	0·000	0·0	1·000	0·017
Aluminium	1	−0·002	0·0000	0·000	0·0	1·000	0·017
Residual	8		0·0054	$6{\cdot}811 \times 10^{-4}$			
Collinearity			−0·0104				
Total			1·1196				

Table 12 Analysis of oxygen (wt-%) variance

O	Degrees of freedom	Predictor coefficient	Sum of squares	Mean squares	F ratio	Probability level	$t_{0.0258} \times$ SE
Mean	1	0·426	2·361	2·361	169·9	0·000	0·075
Sulphur	1	0·134	0·215	0·215	15·5	0·004	0·078
T	1	0·032	0·012	0·012	0·9	0·380	0·078
p	1	−0·005	0·000	0·000	0·0	1·000	0·078
Aluminium	1	−0·065	0·051	0·051	3·7	0·092	0·078
Residual	8		0·112	0·0139			
Collinearity			−0·047				
Total			2·704				

Published by Maney Publishing (c) IOM Communications Ltd

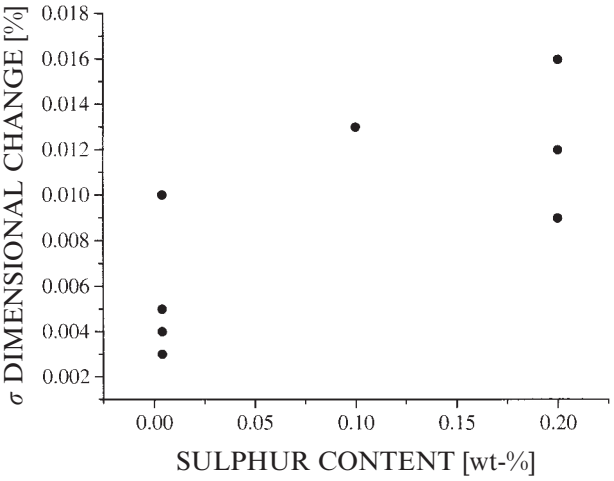

12 Dimensional change standard deviation versus sulphur content

energy of the water as being important as a sine term was added to the denominator

$$\mu_P = \frac{k}{u_W \sin(\alpha)} \quad . \quad . \quad . \quad . \quad . \quad . \quad . \quad . \quad . \quad . \quad . \quad (5)$$

One observation is that the 48% increase in water pressure and water energy was accompanied by a decrease in particle size by 39%.

The results of the present work suggest an m value in equation (2) equal to 1·25. The speed of the water jets u_w is proportional to water pressure, $u_w = \phi(2p_W/\rho_W)^{1/2}$, where ρ is the density and ϕ is a constant. If the contribution of melt velocity is ignored, the equivalent water pressure exponent m (from equation (2)), would be equal to 0·34 in equation (4). The equivalent water pressure exponent m, equals 0·48 and 0·5 in equation (5). In the present work, equations (3)–(5) underestimate the effect of water pressure. The exponent 0·8 suggested by Dunkley is within the confidence limit, and is proposed here.[22]

Sulphur

It is shown that there is a sulphur effect on particle size as particle size decreased with large sulphur additions. This is in accordance with the presumed surface tension effect, but also in accordance with the presumed viscosity effect.[25] The experiment does not allow for a direct determination whether surface tension or viscosity is responsible for the reduced particle size. The effect of sulphur additions up to 0·2 wt-% is small and would not have been detected as active if the effects were calculated on these and zero addition runs alone. For the largest addition, a reduced particle size was clearly seen. The maximum effect of sulphur on viscosity reported by Frohberg and Cakici[18] was seen already at 0·1 wt-%S, an addition that did little to alter particle sizes of the powder. As only the highest sulphur level notably lowered particle size, this shows that viscosity has little effect, as do other investigations where surfactants had little effect on the viscosity.[14]

If the effect of an addition of 1·5 wt-%S is a surface tension effect, an estimate based on binary iron–sulphur investigations would have concluded that the surface tension for 0·2 wt-%S would be approximately 45% lower than for a pure melt (Fig. 1). A further increase in sulphur content to 1·5 wt-% would lower the surface tension to an additional 20%. Thus, most of the decrease in particle size would have occurred already at 0·2 wt-%S.

According to calculations in the Appendix, the diffusion rate of sulphur is sufficient for equilibrium segregation of sulphur to the surface of the droplets to take place. The water jet consists of only 2 vol.-% water,[22] the rest being steam or gas sucked into the jet. If the jet contains enough oxygen to lower the surface tension, only very high sulphur contents would lower it further (Fig. 1). This was seen in the present work as well, indicating that the particle size effect owing to the high sulphur addition is a surface tension effect.

The different behaviour of water atomisation compared with gas atomisation is thus the atomising medium. The water jets lower surface tension and make the process robust against alloying impurities. The oxygen effect should also explain the smaller particle sizes seen when the atomising chamber is filled with air instead of protective atmosphere.[29]

The linear particle size model, equation (1), predicts that 1·5 wt-%S would reduce the diameter of a 78·74 μm particle by 22%, thus the area of formed particles increases by 29%, calculated as if the particles were spherical. Surface tension measurements of Fe–O melts are limited to oxygen

Table 13 Analysis of carbon (wt-%) variance

C	Degrees of freedom	Predictor coefficient	Sum of squares	Mean squares	F ratio	Probability level	$t_{0·0258} \times$ SE
Mean	1	0·204	0·5402	0·5402	76·1	0·000	0·054
Sulphur	1	−0·002	0·0001	0·0001	0·0	0·908	0·056
T	1	0·002	0·0001	0·0001	0·0	0·908	0·056
p	1	−0·029	0·0098	0·0098	1·4	0·274	0·056
Aluminium	1	0·067	0·0537	0·0537	7·6	0·025	0·056
Residual	8		0·0566	0·0071			
Collinearity			0·0013				
Total			0·6617				

Table 14 Analysis of nitrogen (wt-%) variance

N	Degrees of freedom	Predictor coefficient	Sum of squares	Mean squares	F ratio	Probability level	$t_{0·0258} \times$ SE
Mean	1	0·022	0·0064	0·0064	40·5	0·000	0·008
Sulphur	1	0·001	0·0000	0·0000	0·0	1·000	0·008
T	1	−0·005	0·0003	0·0003	1·9	0·205	0·008
p	1	−0·005	0·0003	0·0003	1·9	0·205	0·008
Aluminium	1	−0·008	0·0009	0·0009	5·7	0·044	0·008
Residual	8		0·0013	$1·579 \times 10^{-4}$			
Collinearity			0·0003				
Total			0·0094				

Published by Maney Publishing (c) IOM Communications Ltd

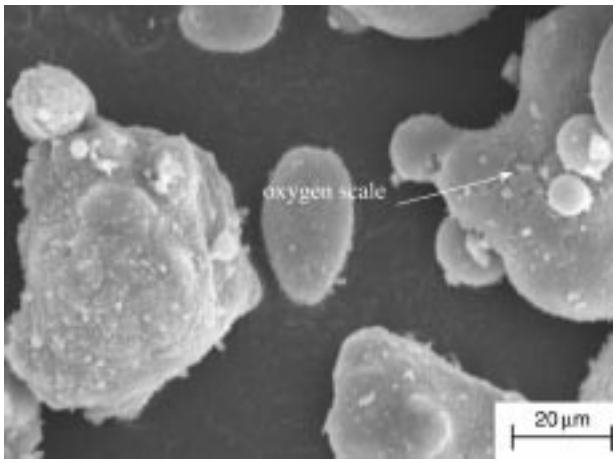

13 Micrograph of particles from F102

concentrations up to 0·1 wt-%. It is reasonable to suspect that it is difficult to reach concentrations beyond this range. At this concentration, surface tension would be around 1·1 Pa. Surface tension of Fe–S alloys at 1·5 wt-%S is near 0·8 Pa. This difference is comparable to the difference of the surface area of the formed particles, assuming spherical shapes.

If the reduced particle size is an effect of reduced surface tension, and if the surface tension is reduced by 30%, the particle size μ_P is proportional to the surface tension raised to the power of 0·8. Since the error bands of the sulphur effect is almost as large as the effect itself, the error bands of the exponent estimate is even larger. Klar and Shafer water atomised copper with different oxygen contents.[8] With increasing oxygen content, the resulting particle size decreased from 38 μm at an O content of 0·02 wt-%, down to 33·2 μm at 0·55 wt-%O, supporting the presumption that surface tension and/or viscosity are/is important.

Comparing the models, in equation (2) μ_P is proportional to $\gamma_M^{-0.15}$ and in equation (3) it is proportional to $\gamma_M^{0.22}$. From the exponent, it is clear that the model by Kishidaka is in better agreement both with current results and with the results of Klar and Shafer, but the exponent seems to underestimate the surface tension effect. In the present work, it is proposed to be 0·8.

Similar to the effect on particle size, run F102 was the only experiment suggesting an oxygen content increase when sulphur was added; contrary to the particle size effect, the oxygen effect was unexpected. As oxygen is also a strong surfactant, it cannot be excluded that the sulphur effect seen was brought about by an increased oxygen uptake, owing to the sulphur additions. The powder from this run was heavily oxidised with visible oxygen scales (Fig. 13).

Temperature

The temperature effect was present, with and without sulphur. A presumption made about the temperature was that there could be an interaction between it and sulphur content. In Fig. 4, the estimated particle size when the water pressure effect was removed is plotted versus melt temperature. The sulphur content of each experiment is indicated by the greyscale of the dots. If a negative temperature–sulphur content interaction existed, higher temperatures would reduce the sulphur effect, and this is not seen, as the effect of the 1·5 wt-%S addition was present at one of the highest investigated temperatures.

The modest temperature difference had a comparatively large impact on particle size. An increase in temperature from 1570 to 1640°C in equation (1) would reduce particle size by 16%. The largest reduction of surface tension that may be assumed to be a result of this temperature change can be calculated with the temperature coefficient obtained for pure iron. The temperature coefficient $d\gamma/dT$ has been established to be −0·34 mPa, which for an oxygen saturated melt with a surface tension of approximately 1 Pa at 1570°C, would mean a reduction of surface tension of 2·4% when the temperature is raised to 1640°C.[4] For the surface tension measurements with surfactants, the temperature coefficient has been reported to increase and ultimately change sign, and if this is true for water atomisation, surface tension would be larger at the higher temperature.

In the same temperature interval, a reduction of viscosity of approximately 10% could be expected.[6] The larger change of the viscosity compared with surface tension would easily explain the difference observed in particle size. In equation (3), μ_P is related to $v_M^{0.35}$ and in equation (4) to $v_M^{0.57}$. Assuming that the temperature effect seen is a viscosity effect, equation (4) is in better agreement with

Table 15 Analysis of dimensional change (%) variance

Dimensional change	Degrees of freedom	Predictor coefficient	Sum of squares	Mean squares	*F* ratio	Probability level	$t_{0.0258} \times$ SE
Mean	1	0·541	2·635	2·635	6244·1	0·00	0·0131
Sulphur	1	0·015	0·002	0·002	4·7	0·10	0·0137
T	1	−0·002	0·000	0·000	0·0	1·00	0·0137
p	1	−0·072	0·042	0·042	99·5	0·00	0·0137
Aluminium	1	−0·009	0·001	0·001	2·4	0·20	0·0137
Residual	4		0·002	$4{\cdot}220 \times 10^{-4}$			
Collinearity			0·000				
Total			2·681				

Table 16 Analysis of dimensional change standard deviation (%) variance

σ_D	Degrees of freedom	Predictor coefficient	Sum of squares	Mean squares	*F* ratio	Probability level	$t_{0.0258} \times$ SE
Mean	1	0·0089	$7{\cdot}15 \times 10^{-4}$	$7{\cdot}15 \times 10^{-4}$	89·6	0·00	0·0018
Sulphur	1	0·0029	$6{\cdot}55 \times 10^{-5}$	$6{\cdot}55 \times 10^{-5}$	8·2	0·05	0·0019
T	1	0·0007	$3{\cdot}90 \times 10^{-6}$	$3{\cdot}90 \times 10^{-6}$	0·5	0·52	0·0019
p	1	−0·0020	$3{\cdot}31 \times 10^{-5}$	$3{\cdot}31 \times 10^{-5}$	4·1	0·11	0·0019
Aluminium	1	−0·0012	$1{\cdot}18 \times 10^{-5}$	$1{\cdot}18 \times 10^{-5}$	1·5	0·29	0·0019
Residual	4		$3{\cdot}19 \times 10^{-5}$	$7{\cdot}982 \times 10^{-6}$			
Collinearity			$-3{\cdot}50 \times 10^{-6}$				
Total			$8{\cdot}58 \times 10^{-4}$				

Published by Maney Publishing (c) IOM Communications Ltd

current results. Takeda and Minagawa,[29] saw a 50% reduction of particle size for water atomised copper powder when increasing melt temperature from 1100 to 1300°C, a difference accompanied by a 10% decrease in surface tension, but a 30% decrease in viscosity.[30] Taking the surface tension effect, with the exponent 0·8 found here, into account, the exponent for viscosity would have to be 2 in order for such a large reduction of particle size to occur. In this experiment, an exponent of 1·35 would be the best estimate. Owing to the large errors involved, the proposed viscosity exponent is 1, a more conservative estimate closer to equations (3) and (4).

Proposed water atomisation model

A modified formula is proposed, based on equations (1) and (2), with the adjusted exponent for water pressure, and considering also the effect of impacting angle, agreed upon by both equations (3) and (5)

$$\mu_P = k \frac{\gamma_M^{0\cdot8} v_M}{p_W^{0\cdot8} \sin \alpha} \left(\frac{G_W}{G_M} \right)^{-0\cdot043} \quad \ldots\ldots (6)$$

The water/metal ratio term is from equation (4). The exponent is small, and this is consistent with the observation that small water/metal ratios lead to coarser powders, but ratios above 6:1 appear to have a small influence on particle size.[22]

Powder size standard deviation results

The standard deviation of the size distribution was smaller for aluminium additions and for melts with high superheats. It is well known that water atomisation of melts with high contents of elements forming strong oxides often exhibit narrow size distributions. Standard deviations of Fe–Si and Ni–Cr–B–Si alloys may be as low as 1·6–1·8, and it is speculated that compounds formed on particle surfaces are responsible for this.[22] Alumina is stable at the atomising temperature, it is not water soluble, and would thus remain on solidified powder if alumina surface layers were responsible for such behaviour. Powders with added aluminium were studied with AES and XPS (ESCA) electron beam analysis, but no trace of aluminium was found on the surfaces, only a FeO scale approximately 150 nm in thickness. Alumina particles are probably formed in the interior as a result of internal oxidation. A speculation consistent with the agglomeration theory is that formed alumina particles permit a faster freezing by acting as inoculants. The requirements for internal oxidation (a high diffusion rate of the oxygen and a low aluminium concentration) are fulfilled. A temperature dependence, as suggested by Fig. 4*b*, is consistent with findings of other researchers.[31,32]

Powder chemistry

No effect on powder oxygen content was seen as a result of aluminium additions or argon practice during melting. This is probably because oxygen pickup mostly occurs after droplets have formed, something also seen when sieve profiles where analysed; only oxygen content differed notably between small and large size fractions. The decrease of nitrogen content seen for deoxidised powders could be a result of aluminium nitrides being formed in the melt, or because the protective argon atmosphere prevented nitrogen pickup. Nitrogen pickup would occur during melting.

Except for run F74, the analysed carbon content was lower for melts molten under argon and with aluminium added. Lowered oxygen content induced by aluminium and by melting under argon would lead to less carbon monoxide or dioxide formation. The deviation of run F74 cannot be explained by deviations noted in the laboratory journal, but it is still considered to be an outlier.

Effects on dimensional change

The reduced swelling exhibited for powders manufactured with high water pressure should reflect an increased sintering rate owing to the larger surface/volume ratios for these powders. The increased standard deviation seen for powders with added sulphur is questionable; it is probably a random effect.

SUMMARY

The energy required to create new surface area when a melt is comminuted into particles is related to the surface tension and viscosity of the melt. In the investigation, influences of surface active elements that greatly influence the surface tension of a melt, are studied regarding their effect on water atomisation. The investigation was performed by varying aluminium content, melting under argon or under air, melting iron powder or pure iron, and by adding sulphur. The studied responses include particle size distribution, apparent density and flow of the powder, carbon, sulphur, oxygen, and nitrogen powder content, and dimensional change of reduced powders admixed with 2 wt-%C and 0·5 wt-% graphite.

The results show that surfactants had small effects compared with the change of water pressure. A higher superheat of the melt also reduced the particle size. There was an effect of a 1·5 wt-%S addition on mass median particle size, and it is concluded to be a result of change in surface tension, but smaller additions did little to change particle size distribution. Higher water pressures also resulted in powder with lower apparent density, lower flowrate, and reduced swelling during sintering. Aluminium additions reduced powder size standard deviation and increased carbon content of the powder.

CONCLUSIONS

The particle size was reduced for additions of sulphur, and this is related to the decrease in surface tension. The effect was seen only with large additions, and it is concluded that oxygen within the water jet already lowers surface tension enough to engulf any effects of trace amounts. This would be especially true when atomising in air.

A narrowed powder size distribution was noted for runs with aluminium additions. It is speculated that inner oxidation and heterogeneous nucleation were responsible for this behaviour.

Aluminium additions and protective atmosphere during melting resulted in powder with more carbon and lower nitrogen content. It is concluded that carbon loss occurred during melting in air, and that aluminium nitrides formed might explain the lower nitrogen content.

The exponent for water pressure in equation (2) is concluded to lie in the range of 0·8–1. It is also concluded that the exponent for surface tension is positive, as in equation (4).

APPENDIX

The small effects of sulphur on particle size and on surface tension may be analysed in terms of cooling rate and diffusion, in order to estimate how much of the sulphur may accumulate on the surface of a spherical droplet. The prevailing disintegration mechanism theory, originally suggested by Grandzol[27] for water atomisation, is that the melt is broken up by impacts of water droplets. Subsequent impacts split the melt droplets until solidification.[33] Until the droplets have solidified, agglomeration of melt droplets may occur.

A general assumption can be made that the diameter of the droplet investigated is 100 μm. Thus, it has approximately twice the volume of a droplet equal in size to the average size from the laboratory experiment (sieve analysis). This droplet is selected as it is interesting to see whether

Published by Maney Publishing (c) IOM Communications Ltd

or not this droplet will split into two or more droplets before solidification. A second general assumption can be made about the maximum surface coverage Γ_S^0. This is reported for the iron–sulphur system as ranging between different investigations from 6·4 to $8{\cdot}9 \times 10^{18}$ atoms per m^2 (Ref. 4). First, the droplets must be checked to see if they contain enough sulphur for surface coverage. Solute atoms available N_{AVAIL} and required N_{REQ} for one monolayer coverage could be expressed as

$$N_{REQ} = \Gamma_S^0 \pi d^2$$

$$N_{AVAIL} = \frac{C\pi d^2}{6}$$

where d is the spherical droplet diameter. The sulphur concentration in atoms per m^3 C could be expressed as

$$C \approx \frac{c_{solute} N_A \rho_M}{100 M_M}$$

where c_{solute} is the sulphur concentration (at.-%), N_A is Avogadro's number (mol), ρ_M is metal density ($g\,m^{-3}$), and M_M is the atomic mass of the metal ($g\,mol^{-1}$). A droplet would have to have a size of d_{min} (m) to contain as much sulphur atoms as required to cover the surface, where d_{min} is given by

$$d_{min} \approx \frac{600 \Gamma_S^0 M_M}{c_{solute} N_A \rho_M}$$

where d_{min} is the minimum droplet size where the sulphur atoms of the bulk equal the number required for complete surface coverage (m). With a liquid iron density of $7{\cdot}06 \times 10^6$ g m^{-3} (Ref. 33) and a sulphur concentration of 0·32 at.-% then

$$d_{min} \approx \{600 \times (7{\cdot}65 \times 10^{18}) \times 55{\cdot}85/[0{\cdot}32 \times (6{\cdot}022 \times 10^{23}) \times 7{\cdot}06 \times 10^6)]\}$$

which is $\approx 0{\cdot}2\ \mu m \ll 100\ \mu m$.

If temperature change effects are ignored, the energy needed to be transported from a 100 μm particle for solidification is

$$Q = \frac{L_f \pi d^3}{6}$$

where L_f is latent heat of fusion ($J\,m^{-3}$). Heat is retracted with a heat flow $\dot{q}$ of

$$\dot{q} = k_T \pi d^2$$

where k_T is the heat transfer coefficient of a water droplet ($W\,m^{-2}$). Thus, time needed to solidify the droplet is

$$t = \frac{L_f d}{6k}$$

The heat transfer coefficient k_T of a water jet, with a water pressure of 12 MPa, impinging a liquid iron droplet with a diameter of 100 μm at 1600°C is 3×10^8 W m^{-2} (Ref. 33). The heat of fusion of iron L_f is 1737 MJ m^{-3}. The heat of fusion would thus be retracted in $\{(1737 \times 10^6) \times (100 \times 10^{-6})/[6 \times (3 \times 10^8)]\} = 96$ μs. With a diffusivity of sulphur in liquid iron at 1600°C, taken as $D = 10^{-8}\ m^2\,s^{-1}$ used by Norell,[34] the average diffusion distance could be approximated as $2(Dt)^{1/2} = 2[10^{-8} \times (96 \times 10^{-6})]^{1/2} \approx 2\ \mu m \gg d_{min}$. The diffusivity range found by Norell from several authors, is from 10^{-9} to $3 \times 10^{-8}\ m^2\,s^{-1}$, with the low value of 10^{-9} taken as the diffusivity $2(Dt)^{1/2} = 2[10^{-9} \times (96 \times 10^{-6})]^{1/2} \approx 0{\cdot}62\ \mu m \gg d_{min}$. If the energy retraction of the temperature decrease is added the time would increase even further. Diffusion alone should not hinder surface coverage. From this simple calculation, it is evident that diffusion will be enough to establish near equilibrium conditions for the sulphur coverage of this droplet.

ACKNOWLEDGEMENTS

The Swedish National Board for Industrial and Technical Development has financed the project under grants No. 95–06473 and 95–11037. The author acknowledges Professor T. Ericsson for work done on this paper, and to A. Köhler-Hanno for proofreading. The author also wishes to thank Höganäs AB for the use of their facilities, and T. Lindström and B. Haase, Höganäs AB, for assistance during the experimentation and for comments on the work. N. Larsson should also be recognised for help with SEM measurements.

REFERENCES

1. A. SALAK: 'Ferrous powder metallurgy'; 1995, Cambridge, Cambridge International Science Publishing.
2. W. STASKO and K. PINNOW: 'Sulphur containing powder metallurgy tool steel'; Crucible Materials Corporation, Syracuse, NY, USA, 1996.
3. T. IIDA and Y. SHIRAISHI: 'Handbook of physico-chemical properties at high temperatures', (ed. Y. Kawai and Y. Shiraishi), 93–120; 1989, The Iron and Steel Institute of Japan.
4. B. J. KEENE: 'A survey of extant data for the surface tension of molten iron and its binary alloys', National Physical Laboratory, Teddington, Middx., UK, 1983.
5. B. C. ALLEN: in 'Liquid metals: chemistry and physics', (ed. S. Z. Beer), 161–212; 1972, New York, NY, Marcel Dekker.
6. T. IIDA and R. I. L. GUTHRIE: 'The physical properties of liquid metals'; 1988, Oxford, Clarendon Press.
7. J. T. STRAUSS: 'Advances in powder metallurgy and particulate materials'; 1993, Princeton, NJ, MPIF.
8. E. KLAR and W. M. SHAFER: *Int. J. Powder Metall.*, 1975, **11**, (4), 241–245.
9. E. KLAR and J. W. FESKO: 'Progress in powder metallurgy'; 1982, Princeton, NJ, MPIF.
10. W. B. LAIRD: 'Method of converting molten metal to powder having low oxygen content', Air Reduction Company, New York, NY, 1970.
11. M. D. AYERS: 'Apparatus for producing low oxide metal powders', Metal Innovations Inc., Stamford, CN, USA, 1974.
12. I. JIMBO, A. SHARAN, and A. W. CRAMB: Proc. 76th Steelmaking Conf., Dallas, TX, March 1993, Iron and Steel Society, 485–494.
13. D. Y. POVOLOTSKY, A. I. STROGANOV, and A. V. PUZYREV: *Izv. Akad. Nauk. SSSR, Met.*, 1971, **4**, (4), 87–90.
14. Yu. A. BAZIN *et al.*: *Izv. V.U.Z. Chernaya Metall.*, 1985, **9**, (9), 16–20.
15. Y. OGINO, F. O. BORGMANN, and M. G. FROHBERG: *Trans. Iron Steel Inst. Jpn*, 1974, **14**, (2), 82–87.
16. V. TSEPELEV *et al.*: *Izv. V.U.Z. Chernaya Metall.*, 1984, **1**, (4), 1–4.
17. N. E. BODAKIN *et al.*: *Russ. Metall.*, 1977, **2**, 59–61.
18. M. G. FROHBERG and T. CAKICI: *Arch. Eisenhüttenwes.*, 1978, **49**, (5), 229–230.
19. N. R. DRAPER and H. SMITH: 'Applied regression analysis'; 3rd edn; 1998, New York, NY, Wiley.
20. D. C. MONTGOMERY and E. A. PECK: 'Introduction to linear regression analysis', 2nd edn; 1992, New York, NY, Wiley.
21. R. H. MYERS: 'Classical and modern regression with applications'; 1986, Boston, MA, Duxbury Press.
22. J. J. DUNKLEY: in 'Metals handbook', Vol. 7, 35–52; 1998, Materials Park, OH, ASM International.
23. A. J. ALLER and A. LOSADA: *Powder Metall. Sci. Technol. (India)*, 1991, **2**, (2), 13–37.
24. Yu. F. TERNOVOY *et al.*: in 'PM '94: World Congress on Powder Metallurgy'; 1994, Les Ulis, Les Editions de Physique, 325–328.
25. H. KISHIDAKA: Proc. Multidisciplinary Meeting on 'Sintered metals and magnetic properties'; February 1972, Japan Society for Powder and Powder Metallurgy, 19–24.
26. R. J. GRANDZOL and J. A. TALLMADGE: *AICHE J.*, 1973, **19**, (6), 1149–1158.
27. R. J. GRANDZOL: in 'Chemical engineering', 273; 1973, Philadelphia, PA, Drexel University.
28. R. J. GRANDZOL and J. A. TALLMADGE: *Int. J. Powder Metall.*, 1975, **11**, (2), 103–114.
29. T. TAKEDA and K. MINAGAWA: *J. Jpn Soc. Powder Metall.*, 1978, **25**, (7), 1–6.

Published by Maney Publishing (c) IOM Communications Ltd

30. C. J. SMITHELLS: 'Smithells metals reference book', 14-6–14-7; 1992, Oxford, Butterworth-Heinemann.
31. Y. SEKI *et al.*: *Met. Powder Rep.*, 1990, **45**, (1), 38–40.
32. J. J. DUNKLEY and J. D. PALMER: *Powder Metall.*, 1986, **29**, (4), 287–290.
33. A. J. YULE and J. J. DUNKLEY: 'Atomisation of melts', 397; 1994, Oxford, Oxford University Press.
34. M. NORELL: 'Influence of segregants on creep fracture of powder metallurgical steel'; 1996, Göteborg, Chalmers University of Technology.

Growth and Processing of Electronic Materials

Edited by
Neil McN. Alford

This volume comprises papers and posters given at the Materials Congress '98 in the workshop 'Growth and Processing of Materials for Electronics'. The area of materials for electronics is strong in the UK. It is far stronger than its profile within the materials community suggests. The impetus for the Growth and Processing session came from the Electronic Applications Divisional Board of The Institute of Materials. The organising committee were Professor Arthur Willoughby, Dr Eric Yeatman, Dr Caroline Millar and Professor Neil Alford. Dr Sue Dunkerton and Professors Colin Humphreys, Peter Goodhew, Roger Whatmore and Nihal Sinnadurie made up the advisory committee. However, the success of the workshop arose from the enthusiasm of the contributors. The range of topics is both broad and of high quality. The processing includes thin film, thick film (mixed oxide and sol-gel) and bulk mixed oxide methods. Professor Don Pashley opened the session with an invited talk on epitaxy growth mechanisms. Achieving epitaxy in electronics applications is sometimes absolutely essential and this lecture demonstrated the science of the processes. The workshop covered an enormous range of materials. The materials include relaxor ferroelectrics, piezoelectrics, dielectrics, superconductors and semiconductors. The applications include infra-red detectors, dielectric resonators, micro-actuators and humidity sensors. There were interesting new structures for piezoelectrics from Birmingham University, some beautiful microscopy from Liverpool and Durham, interesting applications of electron energy loss spectroscopy from Cambridge. Dielectric resonator materials and superconductors were covered by South Bank and by Leeds who have a strong tradition in electroceramics. There were papers on preparation and characterisation of both piezoelectrics and relaxor ferroelectrics. Piezoelectric thin films made by combining liquid metal precursors were described by Imperial College. Solar cell research was described by both Liverpool and Cranfield. Industrial activity on Cd–Hg–Te infra-red detectors was described by GEC Marconi Infra-Red Ltd and there was a down-to-earth paper on packaging from TWI.

B703 ISBN 1 86125 072 X Hbk 144pp
European Union £45/Members £36
Non-European Union $90/Members $72
p&p European Union £5.00/Non-EU $10.00 per order

Orders to: IOM Communications Ltd, Shelton House, Stoke Road, Shelton, Stoke-on-Trent ST4 2DR Tel: +44 (0) 1782 202 116 Fax: +44 (0) 1782 202 421
Email: Orders@materials.org.uk Internet: www.materials.org.uk

IOM Communications
IOM Communications Ltd is a wholly-owned subsidiary of the Institute of Materials

Published by Maney Publishing (c) IOM Communications Ltd